

Temperature dependence of intersublevel absorption in InAs/GaAs self-assembled quantum dots

F. Bras, P. Boucaud,^{a)} S. Sauvage, and G. Fishman

Institut d'Électronique Fondamentale, UMR CNRS 8622, Bâtiment 220, Université Paris-Sud, 91405 Orsay, France

J.-M. Gérard

CEA-Grenoble, DRFMC-PSC, 38054 Grenoble Cedex 9, France

(Received 6 February 2002; accepted for publication 24 April 2002)

We have studied the temperature dependence of the intersublevel absorption in *n*-doped InAs/GaAs self-assembled quantum dots. The investigated intersublevel transition corresponds to the optical transition between the *s*-type conduction ground state to the *p*-type first excited states. These transitions, resonant between 20 and 22 μm , are in-plane polarized along the $[110]$ and the $[\bar{1}10]$ directions. A redshift lower than 3 meV is observed for the transition resonance from low temperature to room temperature. While the effective barrier height from the ground state is around 150 meV, the integrated absorption amplitude decreases by a factor of 4 from low temperature to room temperature. This decrease is modeled by the thermionic emission of the carriers, taking into account the density of states of the two-dimensional wetting layer, the density of states of the three-dimensional bulk layer surrounding the dots and the existence of polaron states associated with the strong electron-phonon coupling in the dots. © 2002 American Institute of Physics.

[DOI: 10.1063/1.1487446]

Optical transitions between conduction confined states or valence confined states of quantum dots can be observed in the infrared spectral range. These transitions are usually referred to as intraband or intersublevel transitions, by analogy with intersubband transitions which are observed in semiconductor quantum wells. The intersublevel transitions can be experimentally observed by charge modulation spectroscopy,¹ photoinduced spectroscopy,² or by direct spectroscopy of doped quantum dots.³

In this letter, we report on the analysis of the intersublevel absorption as a function of the temperature. We have studied the intersublevel absorption between the quantum dot *s*-type ground state to the first *p*-type excited states in *n*-doped InAs/GaAs self-assembled quantum dots. A spectral redshift of the intersublevel resonance lower than 3 meV and a decrease by a factor of 4 of the integrated absorption are observed from low temperature to room temperature. This temperature dependence is modeled by considering the density of states of the continuum and the existence of polaron states which result from the strong electron-phonon coupling in the dots.

The investigated sample was grown by molecular beam epitaxy.³ It consists of 30 InAs quantum dot layers separated by 50-nm-thick GaAs barriers. The dot density, as estimated from separate atomic force microscopy measurements, is around $4 \times 10^{10} \text{ cm}^{-2}$. A nominal doping of two carriers per dot was provided by a delta-planar modulation doping 2 nm below the quantum dot layers. The dots have a flat elliptical lens-shaped geometry with a typical dot height of 2.5 nm and a base length of 25 nm. The intersublevel absorption was measured in a normal incidence configuration geometry with

a Fourier-transform infrared spectrometer. The transmission of the sample was normalized by the transmission of a reference bulk GaAs sample with a similar thickness. This normalization of the transmission is particularly sensitive to the thickness of the samples as the intersublevel absorption is close in energy to a two-phonon absorption of the substrate.

Figures 1(a) and 1(b) show the temperature dependence of the intersublevel absorption measured along the $[\bar{1}10]$ and the $[110]$ directions, respectively. At low temperature, the transitions are resonant at 56 and 63 meV with a broadening ~ 6 meV at full width at half maximum. The absorption corresponds to the transitions from the quantum dot ground state to the first excited states. The splitting between the intersublevel transitions is a consequence of the dot elongation along the $[\bar{1}10]$ direction (see for instance Ref. 4). The electronic structure of the quantum dots was calculated by solving the three-dimensional Schrödinger equation written in a eight band $\mathbf{k}\cdot\mathbf{p}$ formalism.⁵ The strain tensor is assumed constant within the InAs dot volume and equal to the one of an InAs quantum well grown on a GaAs substrate. The GaAs barriers are assumed unstrained. The core of the quantum dots consists of pure InAs. The confinement energy of the ground *s*-type state and the first excited *p*-type states of a $25 \text{ nm} \times 28 \text{ nm} \times 2.5 \text{ nm}$ elliptical quantum dot leads to in-plane polarized intersublevel transitions from the ground state resonant at 56 and 63 meV. The dipole matrix elements for these transitions are 3.4 and 3.2 nm, respectively. Additional *d*-type excited states are calculated at 115, 121, and 128 meV above the ground state.⁶ The confined states start to hybridize with the wetting layer at 160 meV above the ground state. Experimentally, a broad asymmetric infrared absorption polarized along the *z* growth axis associated with the transition from the ground state to the two-dimensional continuum was observed at room temperature with a resonance around 150

^{a)}Electronic mail: phill@ief.u-psud.fr

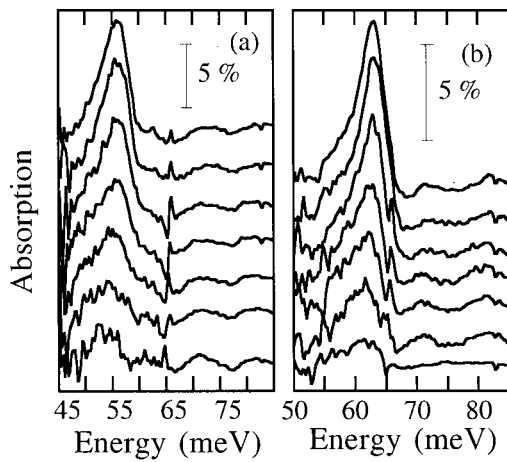


FIG. 1. (a) Intersublevel absorption measured at normal incidence along the $[\bar{1}10]$ direction as a function of the temperature. From top to bottom: 15, 60, 110, 160, 210, 250, and 290 K. (b) Same measurement along the $[110]$ direction. From top to bottom: 15, 60, 110, 160, 210, 250, and 290 K.

meV.³ The three-dimensional continuum state originating from the surrounding GaAs barrier is expected at higher energy by about 30 meV, as deduced from photoinduced experiments on undoped samples.⁷ The average dot population can be deduced from the amplitude (8.8%) and the broadening (3 meV half width at half maximum) of the absorption and from the calculated dipole matrix elements. At low temperature, an average carrier concentration of 1.2 carriers per dot is deduced from the measurement. It is worth noting that when a carrier is thermally excited on the p state, it still contributes to the absorption through transitions from p states to d states with an energy close to that of the $s-p$ transition and with a similar dipole matrix element.

Figure 2 shows the temperature dependence of the peak resonance energy of both intersublevel transitions as a function of the temperature. A weak dependence of the resonance energy vs temperature is observed as illustrated by a redshift lower than 3 meV from low temperature to room temperature. This nonlinear redshift is similar to the one reported in the case of intersubband transitions in quantum wells.⁸ We do not observe a significant variation of the linewidth of the transition. A direct comparison between intersublevel absorption and intersubband absorption is not straightforward as the temperature dependence of intersubband transitions significantly depends on the doping density.⁹ Different thermal be-

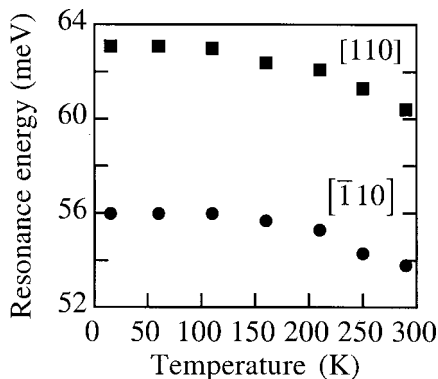


FIG. 2. Energy resonance of the intersublevel absorptions as a function of the temperature. squares $[110]$ direction; full dots $[\bar{1}10]$ direction.

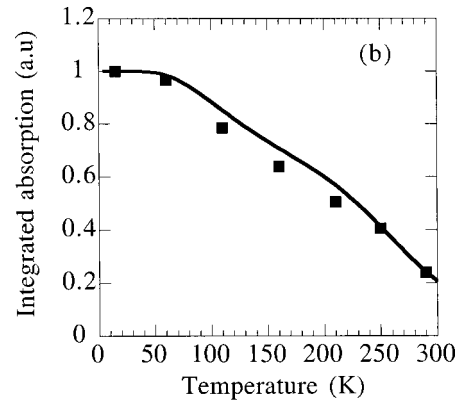
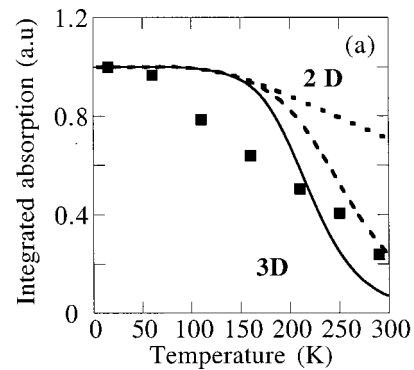


FIG. 3. (a) Normalized integrated intersublevel absorption as a function of the temperature (squares). The dotted line corresponds to the calculated intersublevel absorption by accounting for a two-dimensional continuum. The dashed and full lines account for a three-dimensional continuum. The calculation is performed with two different dot three-dimensional carrier densities ($8 \times 10^{13} \text{ cm}^{-3}$ —dashed line and $2 \times 10^{13} \text{ cm}^{-3}$ full line). The effective barrier height from the ground state to the two (three)-dimensional continuum is 0.15 (0.18 eV). The absorption has been normalized to 1 at low temperature. (b) Intersublevel integrated absorption (squares) and population of the ground state (full line) as a function of the temperature calculated by accounting for an intermediate level at 30 meV from the ground state and for the three-dimensional continuum. The three-dimensional dot carrier density is $2 \times 10^{13} \text{ cm}^{-3}$.

haviors for intersubband absorption were also reported between modulation doped and well doped samples.¹⁰

Figure 3(a) shows the temperature dependence of the integrated absorption. A significant decrease by a factor of 4 is observed for the amplitude of the integrated absorption from low temperature to room temperature. This decrease is stronger than its expected value $\exp(-E_a/kT)$ for an activation energy E_a to the continuum ~ 150 meV. We note that the onset of the decrease of the integrated absorption occurs at low temperature around 70 K.

To interpret this strong decrease of the absorption, we consider the thermal depopulation of the dots in a single particle picture, assuming that the carrier transfer from the modulation doping to the quantum dots does not depend on temperature. The thermal behavior of the quantum dots offers a strong analogy with the ionization of donors in bulk materials. In the latter case, the larger density of states of the three-dimensional continuum has to be considered in order to understand the ionization. In the following, two distinct cases were considered: the ionization of the dots towards a two-dimensional (2D) continuum or the ionization of the dots towards a three-dimensional continuum. In the case of a

two-dimensional continuum, the Fermi level can be obtained from Eq. (1):

$$N_{qd}^{2D} [1 - 2f(E_1) - 4f(E_2) - 6f(E_3)] = \frac{m^*}{\pi \hbar^2} k_B T \ln \left(1 + \exp \frac{E_F - E_{c1}}{k_B T} \right), \quad (1)$$

where N_{qd}^{2D} is the surface density of dots, $m^* = 0.06 m_0$ is the electron effective mass, E_F is the Fermi level energy, E_{c1} is the energy of the 2D continuum, E_1 the energy of the ground confined state, $f(E_1) = 1/[1 + \exp(E_1 - E_F)/k_B T]$ is the Fermi-Dirac function, E_2 is the energy of the first p -type excited state, E_3 is the energy of the d -type excited states, k_B is the Boltzmann constant, and T is the temperature. For simplicity, the p and d states were considered degenerated in energy with a two-fold and a three-fold degeneracy, not including spin, respectively. In the case of a three-dimensional (3D) continuum, the Fermi level can be derived from Eq. (2):

$$N_{qd}^{3D} [1 - 2f(E_1) - 4f(E_2) - 6f(E_3)] = \int_{E_c}^{\infty} dE \frac{1}{2\pi^2} \left(\frac{2m^*}{\hbar^2} \right)^{3/2} \sqrt{E - E_c} f(E) \quad (2)$$

where N_{qd}^{3D} is the volumic density of dots. Equations (1) and (2) were solved numerically to determine the Fermi level. The absorption is deduced from the quantum dot population by taking into account the dipole matrix elements for the $s-p$ and $p-d$ transitions. The calculations were performed for a single quantum dot layer.

The calculated temperature dependence of the intersublevel absorption is shown in Fig. 3(a) for three distinct cases. The dotted line accounts for the electronic structure of the dots and for a two-dimensional continuum at 150 meV above the ground state. The dashed and full lines account for a three-dimensional continuum at 180 meV above the dot ground state. In the latter cases, three-dimensional dot densities have to be introduced. The *three-dimensional* dot density requires a normalizing volume for the quantum dots, and thus an effective length along the z direction. In an electrostatic picture, the effective length would be associated to the depletion length between the n -doped quantum dot region and the residual p -doped substrate where band bending is observed. Under flatband condition, this effective length corresponds to a length for which the carriers and the dots are in interaction. Starting from a two-dimensional density of 4×10^{10} dots per square centimeter, the three-dimensional densities reported in Fig. 3(a) of $2 \times 10^{13} \text{ cm}^{-3}$, and $8 \times 10^{13} \text{ cm}^{-3}$ correspond to effective lengths $l_c = N_{2D}/N_{3D}$ of 25 and 5 μm , respectively. Figure 3(a) shows that the ionization of the quantum dots directly depends on the three-dimensional density. A large density in the continuum leads to a more efficient thermal ionization at room temperature. Reciprocally, it indicates that quantum dots with a small density cannot be efficiently populated at high temperature.

A three-dimensional dot density of $8 \times 10^{13} \text{ cm}^{-3}$ and a constant barrier height of 0.18 eV lead to a reduction of the intersublevel absorption by a factor of ~ 4 from low temperature to room temperature, in agreement with the experimen-

tal observations. However, the temperature corresponding to the onset of the absorption decrease is around 150 K while it is observed around 70 K experimentally. This feature is attributed to the presence of an intermediate level between the s -type ground state and the p -type first excited state which is a consequence of the strong coupling for the electron-phonon interaction in the quantum dots. This strong coupling leads to the formation of polarons that consist of mixed electron-phonon particles.¹¹ As shown by a calculation on quantum dots similar to those presently studied, this coherent admixture leads to an additional state with a four-fold degeneracy, including spin, at around 30 meV above the ground state.¹² We have thus introduced in the calculation a level with a four-fold degeneracy at an energy of 30 meV above the ground state. Figure 3(b) shows the temperature dependence of the population of the dot ground state, that is compared to the temperature dependence of the intersublevel integrated absorption.¹³ A satisfying agreement is now obtained between simulation and experimental data in this case. We note that the shoulder around 200 K corresponds to the thermal ionization of the carriers towards the three-dimensional continuum. At lower temperature, the carriers are excited towards the higher-lying discrete states in the quantum dots. While the full description of the energy structure of the dots in terms of polarons is beyond the scope of this letter, it explains the onset of the absorption decrease around 70 K. It also emphasizes the importance of the polarons for the study of intersublevel excitations in InAs/GaAs self-assembled quantum dots.

The authors acknowledge R. P. S. M. Lobo for providing the helium-flow cryostat and O. Verzellen for fruitful discussions.

¹H. Drexler, D. Leonard, W. Hansen, J. P. Kotthaus, and P. M. Petroff, Phys. Rev. Lett. **73**, 2252 (1994).

²S. Sauvage, P. Boucaud, F. H. Julien, J.-M. Gérard, and J.-Y. Marzin, J. Appl. Phys. **82**, 3396 (1997).

³S. Sauvage, P. Boucaud, F. H. Julien, J.-M. Gérard, and V. Thierry-Mieg, Appl. Phys. Lett. **71**, 2785 (1997).

⁴Y. Nabetani, T. Ishikawa, S. Noda, and A. Sakaki, J. Appl. Phys. **76**, 347 (1994).

⁵For simplicity, the labelling of the confined states as $s-p$ or d -type states refers to electronic states in a single particle picture and does not directly apply to coherent coupled states like polarons. Note that the intersublevel resonance energies and the dipole matrix elements for these dots are not expected to be significantly modified by the strong electron-phonon coupling.

⁶Optical transitions between p and d states are also in-plane polarized with a dipolar matrix element equivalent to that of $s-p$ transitions.

⁷S. Sauvage, P. Boucaud, J.-M. Gérard, and V. Thierry-Mieg, Phys. Rev. B **58**, 10562 (1998).

⁸M. O. Manasreh, F. Szmulowicz, D. W. Fischer, K. R. Evans, and C. E. Sputz, Appl. Phys. Lett. **57**, 1790 (1990).

⁹G. Gumbs, D. Huang, and J. P. Loehr, Phys. Rev. B **51**, 4321 (1995).

¹⁰P. Von Allmen, M. Berz, G. Petrocelli, F.-K. Reinhart, and G. Harbeke, Semicond. Sci. Technol. **3**, 1211 (1988).

¹¹S. Hameau, Y. Guldner, O. Verzellen, R. Ferreira, G. Bastard, J. Zeman, A. Lemaitre, and J. M. Gérard, Phys. Rev. Lett. **83**, 4152 (1999).

¹²O. Verzellen, R. Ferreira, and G. Bastard, Phys. Rev. B **62**, R4809 (2000).

¹³The calculation is performed for a fixed average barrier height to the 3D continuum of 180 meV. Integrating over the dot size distribution leads to a very similar result as reported in Fig. 3(b).